FOREX Publication
Open Access | Rapid and quality publishing

International Journal of
Electrical and Electronics Research (IJEER)
Research Article | Volume 13, Issue 4| Pages 960-970|e-ISSN: 2347-470X

Compact Folded T-Stub Microstrip Antenna with PIN Diode-Based Switching for Quad-Band Sub-6 GHz Wireless Systems

Jinan N. Shehab[1*], Israa Hazem Ali[2], and Huda I. Hamd[3]
[1]*Department of Communication Engineering, University of Diyala, Diyala, Iraq; Email: jinan_alazawii_eng@uodiyala.edu.iq*
[2]*Department of Communication Engineering, University of Diyala, Diyala, Iraq; Email: Israa_Hassan_Eng@uodiyala.edu.iq*
[3]*Department of Electronic Engineering, University of Diyala, Diyala, Iraq; Email: Huda.Ibrahim@uodiyala.edu.iq*

***Correspondence:** *jinan_alazawii_eng@uodiyala.edu.iq*

ABSTRACT- The article describes a miniaturized design of a microstrip patch antenna for wireless systems operating at frequencies below 6GHz. It consists of one PIN diode that can dynamically switch between two different operation modes without the need for any mechanical alterations to the radiator. The prototype was built on a Rogers RT/Duroid 5880 substrate ($\varepsilon_r = 2.2$, $\tan\delta = 0.0009$). The design has a small footprint of 17 x 17 x 0.55 mm^3. In "OFF" mode, "THS-RA" achieves tri-band (3.34 GHz, 5.347 GHz, 6.409 GHz) and satisfies 5G Sub-6GHz, Wi-Fi 5, and Wi-Fi 6E/Industrial Sensing Standards. In "ON" mode (when the diode is activated), "THS-RA" will convert to a single-band operating frequency of 2.44GHz, used for ISM, Bluetooth, and WLAN applications. Both modes yield reflection coefficients below -10dB and stable realized gains from 0.52dBi to 1.96dBi. The Folded T-Stub Reconfigurable Antenna will operate at multiple frequencies without the need for an externally tuned circuit and can be implemented in compact, low-power multi-standard wireless devices (IOT), as well as future communication systems.

General Terms: Antenna design, compact folded antenna, PIN diode, simulation software.

Keywords: Quad-band reconfigurable antenna, PIN diode control, Sub-6 GHz wireless systems, Multi-state resonance tuning, Compact patch design, Frequency-switchable operation, 5G, WLAN, Wi-Fi 6E integration.

ARTICLE INFORMATION
Author(s): Jinan N. Shehab, Israa Hazem Ali and Huda I. Hamd.
Received: 06/08/2025; **Accepted**: 05/12/2025; **Published**: 30/12/2025;
E- ISSN: 2347-470X;
Paper Id: IJEER250136;
Citation: 10.37391/ijeer.130436
Webpage-link:
https://ijeer.forexjournal.co.in/archive/volume-13/ijeer-130436.html

Publisher's Note: FOREX Publication stays neutral with regard to jurisdictional claims in Published maps and institutional affiliations.

1. INTRODUCTION

As wireless communication technology, such as Wi-Fi, WLAN, and 5G Sub-6 GHz, Internet of Things, is growing explosively, it has created a need for small, flexible antenna systems that can operate on multiple frequency bands in one compact configuration. As a result of the need for spectrum reuse, convergence of devices, and rapid response to application needs, traditional static single-band antennas are no longer suitable for such an ever-changing environment.[1], [2].

Reconfigurable antennas (RAs) are capable of changing their radiation characteristics, such as frequency, polarization, or radiation pattern in real time. As such, RAs represent a robust answer to the challenges posed by these dynamic needs and offers many advantages over other approaches to reconfigurability. Specifically, FRAs (far-field) provide efficient spectral adaptability, while still being very compact and easy to use. This combination of features makes FRAs particularly well suited for the needs of contemporary multi-standard wireless devices.[3].

The usage of PIN diodes as tuning devices has attracted a great deal of interest from designers because with the small size, low cost and fast switching performances in addition to an easy DC biasing. When weighed against RF-MEMS with inherently intricate fabrication and sluggish actuation, or varactor diodes with nonlinearity and a limited tuning range, PIN diodes can achieve a balance between simplicity and versatility [4]. Strategically included in patch or slot structures, a single PIN diode is also capable of enabling discrete frequency reconfigurability by modifying the effective electrical length of the radiating element [5].

Recent advances have proved that PIN diode loaded reconfigurable microstrip antennas may yield dual- or multi-band operations, with low design complexity and good impedance match. These configurations also achieve stable gain and omnidirectional radiation characteristics, which is a critical issue for IoT and Sub-6 GHz wireless communication applications [6], [7]. Further, the adoption of low-cost substrates such as FR-4 or low-loss substrates like Rogers RT/duroid 5880 to suppress backward radiation can largely affect the antenna's characteristics like the radiation efficiency, bandwidth and size in compact reconfigurable configurations [3].

The latest research is directing the design of small, flexible-frequency antennas capable of being dynamically tuned using a

FOREX Publication
Open Access | Rapid and quality publishing
International Journal of Electrical and Electronics Research (IJEER)
Research Article | Volume 13, Issue 4| Pages 960-970|e-ISSN: 2347-470X

PIN-diode switching approach for the broad frequency range of Sub-6 GHz used by 5G networks, WLAN systems, and IoT device types. In the following section, an organized table of some of the selected designs is presented, along with a description of their significant features by operating frequency, reconfiguration technique, substrate material, and gain capabilities.

Nguyen et al. [8] proposed a small-size frequency-reconfigurable antenna with the capability of wideband sensing and narrowband communication for sub-6 GHz 5G cognitive radio. The antenna utilized two PIN diodes and three varactors, making for a tunable range of 3.4–5.32 GHz with gains of 6.02dB (WB) and 5.37dB (NB). Its efficient switching was offset by the complexity and power control of multiple active devices in the system. Then kumari et al. [9] presented a small monopole antenna (35×35×1.6mm³, FR4) with four reconfigurable modes achieved through RF PIN diodes. It operated over 6GHz frequency bands including Wi-Fi (2.4 GHz), Sub-6GHz 5G (3.5 GHz), Vo5G (4.7 GHz), V2X (5.8 GHz) and C-band (6.25 GHz) with low VSWR (<1.5) and many locations achieved the gain of up to 79%. Although functionally versatile, its large size also poses problems with regard to miniaturized platforms.

A frequency-reconfigurable antenna was built in [10] using a FR4 substrate measuring 15×21×1.6 mm^3 with two PIN diodes to offer six working bands. In addition, this antenna could reach wideband, dual band, and triband modes at frequencies ranging from 2.07 GHz to 9.4 GHz while still producing an acceptable omnidirectional pattern and accommodating multi-mode operation. In [11], A small 22 x 22 x 0.762 mm^3 antenna, built on Rogers 5880 substrate and equipped with 4 PIN diodes, has been created to produce multiple bands of operating frequencies from 7.5 GHz-13.6 GHz. It has a peak measured gain of 5.34 dBi with a return loss of -34.73 dB. The high total and radiated efficiency show the antenna's capabilities; however, since it was designed to operate primarily in the higher frequency range, it is not suited for low-power IoT or Sub-6 GHz 5G applications. In [12], Researchers created a DRAGON fractal antenna specifically for use at higher frequencies designated as 5G (N77-N79, N96) which operates between approximately 6-10 GHz. This antenna has been manufactured using FR4 (50x45 x1.6) mm^3 dimensions housing a 6^{th} order nested fractal radiator terminated *via* coplanar waveguides providing an extended frequency range from 3.67-6.70 GHz with maximum gain up to 5.50 dBi. Although this antenna does provide wide-ranging national coverage and an acceptable range of antenna gains over the desired frequency domain, its relatively larger size could hinder its applications in today's compact wireless communication equipment.

Recent advances in wireless technology have created an urgency to create increased spectral agility, compact, and simple hardware for contemporary platforms. In this context, we present a highly compact, frequency reconfigurable microstrip antenna that uses a single PIN diode as a minimalist switch. In fact, this very minimal switching topology allows for a discrete transition from a mono-band mode to quad-band mode, thus giving the user access to four distinct and strategically useful frequency bands (*e.g.*, WLAN, Sub-6 GHz 5^{th} Generation [5G], Wi-Fi5, and Wi-FI6). This design represents a trade-off between simplicity and performance (*i.e.*, stable radiating characteristics, good efficiency with regard to gain, low profile), hence generating a highly scalable, energy-efficient solution for future generations of reconfigurable wireless systems. The following sections describe the design steps, the electromagnetic simulations, and the performance assessment, showing how the proposed antenna compares with earlier designs in terms of practicality and overall capability. This study offers an innovative approach to the design of T-stub antennas by combining compact folded T-stub radiators with a single PIN diode to achieve multi-band reconfiguration without requiring complex switching networks. The folded geometry allows for a long current path to be contained within a small area. The intrinsic capacitive discontinuities along with the modified ground plane work together to provide for the separation and stability of the resonant modes. These two features allow for predictable switching behavior and a more consistent impedance performance, which set the proposed antenna apart from current Sub-6 GHz antenna designs.

2. DESIGN OF THE PROPOSED FOLDED T-STUB RECONFIGURABLE ANTENNA (FTS-RA)

The geometry of the antenna has been carefully designed in order to satisfy three important requirements: compactness, multi band operation and electrical reconfiguration for Sub-6 GHz wireless communication. It is made of a T-shaped open-ended microstrip stub as shown in *fig. 1* (Step 1) that serves as a quarter-wave resonator supporting a high frequency mode at 8.2 GHz. This resonance arises from a strong standing wave that is established by crossing current paths, satisfying [13], [14]:

$$f_r = \frac{c}{\sqrt{\varepsilon_{eff}} 4 L_{eff}} \quad (1)$$

Where *L_eff* represented, the total effective current path traversed along the horizontal and vertical segments of the stub, while *ε_eff* represents the effective permittivity of the guided structure.

To account for the fringing fields that extend beyond the physical boundaries of the microstrip, the effective permittivity is approximated using the well-established relation:

$$\varepsilon_{eff} = \frac{\varepsilon_r + 1}{2} + \frac{\varepsilon_r - 1}{2} \left(1 + 12 \frac{h}{w}\right)^{-\frac{1}{2}} \quad (2)$$

where *ε_r* is the relative permittivity of the substrate, *h* is the substrate thickness, and *w* is the width of the microstrip line.

The geometric parameters of the T-stub are established based on the relationship between the length of the stub and the quarter wave resonance frequency of the desired upper frequency range. The open-end terminations help establish a maximum voltage at both ends of the T-stub to improve the coupling to stand wave modes of resonant frequency without needing the addition of any vias or alterations to the ground plane.

FOREX Publication
Open Access | Rapid and quality publishing
International Journal of Electrical and Electronics Research (IJEER)
Research Article | Volume 13, Issue 4| Pages 960-970|e-ISSN: 2347-470X

In steps 2 through 4 of the design process, we added several additional vertical and horizontal stub circuits to achieve longer effective electrical lengths (L_eff) and generated new resonances in the lower frequency range, again using the quarter-wave technique as described by [15]. The compact curvature of the stubs and the presence of capacitive discontinuities at the sharp corners of the stubs caused the shift in resonance frequency to be naturally less than we expected, and these discontinuities also caused the local phase velocity to be changed, thereby producing the upward shift of resonance frequencies, although we increased the physical length.

The extra material added in *step 4* (*Figure 1*) resulted in a slight improvement in the impedance match at approximately 8.5 GHz by creating a longer surface current path along the vertical stubs of the left side of the model, however, it did not create a new Sub-6 GHz resonance. In *step 5*, the introduction of an open-ended horizontal slot yielded more opportunities to generate folded current loops; thus, new resonances at ~2.5 and ~8.2 GHz were created. Furthermore, while these findings point to the possibility of creating Multi-band operation, the largest resonance occurs above 8 GHz. Therefore, the results suggest that additional (active) tuning circuitry must be implemented to achieve Sub-6 GHz reconfigurable frequencies. Thus, geometric reconfiguration would still be required to realize efficient Sub-6 GHz operations.

The use of a partial ground cut underneath the radiating patch, known as a defected ground structure (DGS), has been employed to create an optimum impedance match and to decrease surface wave losses [13], [14]. The addition of a DGS provides extra inductive and capacitive loading, adjusting the effective guided wavelength and increasing the electromagnetic coupling. Therefore, through the use of the DGS in steps 6 of *Figure 1(a)* and *(b)*, the antenna was able to obtain definitive triple-band responses at 3.34 GHz, 5.347 GHz, and 6.409 GHz with a reflection coefficient of -24 dB or less. The alteration of the current distribution to above mentioned provides a modal purity increase and energy confinement, thus providing a baseline for additional integration of the PIN diode reconfiguration technology. The final antenna geometric configuration is presented in *figure 2*.

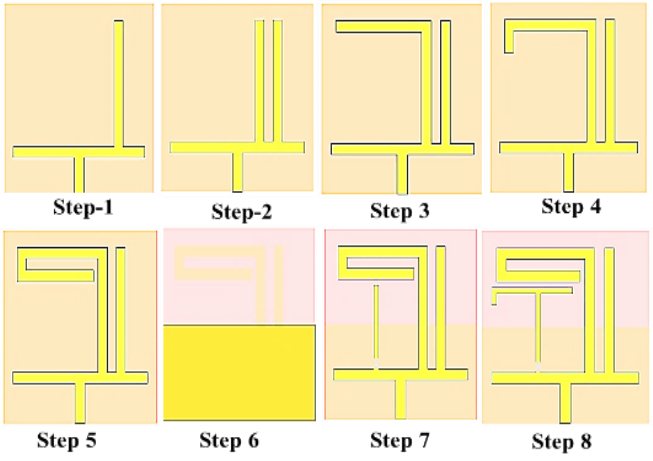

(a)

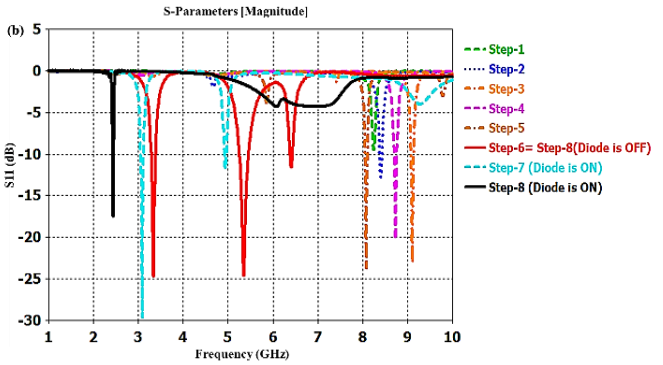

Figure 1. Progressive Design Stages and S_{11} Response of the proposed Folded T-Stub Reconfigurable Antenna (FTS-RA)

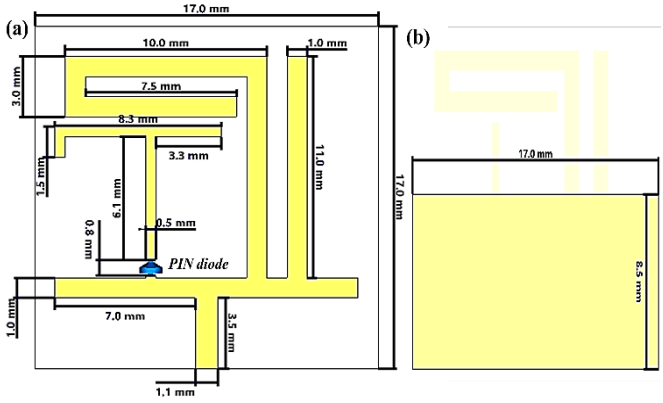

Figure 2. (a) Top view of the proposed Folded T-Stub Reconfigurable Antenna (FTS-RA) with dimensional annotations and integrated PIN diode; (b) Bottom view showing the partial ground plane configuration

3. PIN DIODE-BASED FREQUENCY SWITCHING MECHANISM

Steps 7 and step 8 of *figure 1* detail advancements made to the previously described design that allow for dynamic control of the antenna's operating frequency, as well as obtaining resonance within the 2.4 GHz ISM Band. Both advancements included incorporation of a reconfigurable switching mechanism using a single PIN diode. A vertical stub has been added at the bottom edge of the radiating patch to serve as an extension of the tunable current path. By inserting the PIN diode between the additional stub and the main radiator, two distinct electrical states can be achieved. In the ON state (forward biased), the diode operates as a low-resistance inductor with R_on=0.5 Ω and L_on=0.12 nH, thus providing a continuous conductive path and enhancing the total electrical length of the resonator (illustrated in *figure 3*). Consequently, the primary resonance is shifted to a lower frequency, thus generating a robust operating mode centered at 2.44 GHz. This lower frequency resonance is depicted in *step 8* (Diode is ON) which supports the Harsh Reality of reconfiguration for low-frequency operation with minimal switching topologies.

A reverse-biased PIN diode can also be thought of as a capacitor in the OFF state, where the model for the diode has R_off = 5 KΩ, L_off = 0.12 nH, and C_off = 0.12 pF. The stub becomes

FOREX Publication
Open Access | Rapid and quality publishing
International Journal of Electrical and Electronics Research (IJEER)
Research Article | Volume 13, Issue 4| Pages 960-970|e-ISSN: 2347-470X

electromagnetically isolated from the rest of the antenna when it is OFF, which means that the antenna reverts back to the high frequency operation established in step 6 to step 8 (diode OFF) as shown in *figure 3*.

This controlled shift in the resonant frequency band of the antenna demonstrated how a single PIN diode can control the transition of the antenna from a single frequency band operation to multi-frequency band operation, while retaining the antenna's compact size and stable radiation pattern. The reconfiguration of the antenna meets the bandwidth and frequency allocation requirements for many existing wireless technologies such as the IoT, WLAN, and 5G Sub-6 GHz.

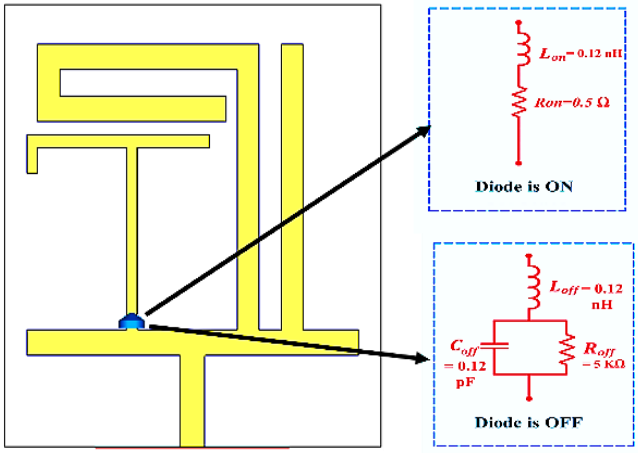

Figure 3. Antenna structure with equivalent circuit models of the integrated PIN diode in ON and OFF states

4. RESULTS AND DISCUSSION

The proposed reconfigurable antenna was implemented on a Rogers RT/Duroid 5880 substrate, chosen for its low dielectric loss and stable electromagnetic behavior. Full-wave simulations were used to examine the design, and even though only one PIN diode was included in the layout, the antenna still demonstrated well-separated multi-band operation. A series of parametric studies to validate the antenna's performance have been conducted, focusing upon the critical geometric dimensions and material parameters. The results of these studies suggest that the antenna is capable of reliably operating within the Sub-6 GHz frequency range with a compact form factor while maintaining a predictable and efficient spectral response.

4.1. S_{11} Characteristics and Frequency Response Across Reconfigurable Switching States

The antenna's electromagnetic performance was evaluated using full-wave simulation methods carried out in CST Microwave Studio Suite 2023. The analysis considered both diode states OFF and ON to capture how the structure reacts when switching between configurations. Fundamental performance measures such as resonant frequencies, return-loss performance (S11), and the overall multiband behavior were used to assess the antenna's spectral response in detail.

Figure 4 shows that in the OFF state the antenna produces three well-separated resonant bands, while in the ON state most of the higher-order modes are suppressed, leaving a single dominant resonance at approximately 2.44 GHz. This transition is controlled by the switching diode, which modifies the current paths and the effective electrical length of the radiator, resulting in a shift of the operating frequency.

S11 simulation values for all modes are less than -10 dB, indicating good impedance matching and low reflection. Movement in the frequency response between different states is primarily due to the effect of the Diode on the effective relative permittivity and on how the boundaries of the structure affect how the mode is distributed. The ability to switch from one mode to another is therefore beneficial for antenna applications, providing flexibility in the spectrum and stable control over the modes of operation. Thus, these antennas can be considered viable candidates for reconfigurable wireless links and sensor-based applications.

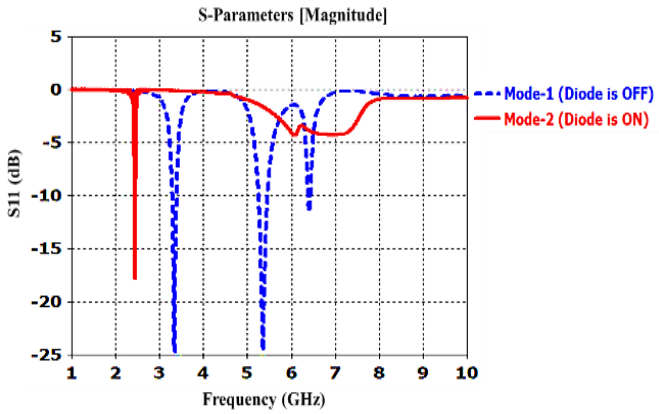

Figure 4. Effect of Switching States on Reflection Coefficient (S_{11}) and Resonant Frequency Reconfiguration

The results demonstrate how robust the antenna design is, and thus, are useful for reconfigurable systems; they have both small size and the ability to be tuned to different frequency ranges, making them appropriate for applications throughout Sub-6 GHz communication standards.

4.2. Parametric Sensitivity Analysis of Geometric Variations

A parametric sensitivity analysis was performed to evaluate the tuning frequency performance for optimal frequency tuning and to determine how consistent that reconfigurable performance is across manufacturing variances. This analysis evaluated three primary geometrical dimensions independently, with the largest being the length of the primary stub (L_1), the width of the top strip (w_1), and the width of the center slot (wd_1). The S_{11} simulations are shown for each of these dimensions in *figure 5(a)-5(f)*, which show how the S_{11} responses of simulated diode devices change with each dimension while keeping the other dimensions constant.

Effect of Stub Length (L_1): The graphs presented as *figures 5(a)* and *figure 5(b)* show how changing L_1 has a large effect on the resonant modes of the antenna. In the OFF position, as L_1 is increased, both the second and third resonant frequencies shift downward which indicates that L_1 dictates how higher order

FOREX Publication
Open Access | Rapid and quality publishing
International Journal of Electrical and Electronics Research (IJEER)
Research Article | Volume 13, Issue 4| Pages 960-970|e-ISSN: 2347-470X

modes are formed in an antenna by providing greater lengths of wire for current flow. In the ON position, L_1 primarily affects the second resonance at about 6.7 GHz, and the lower frequency main resonances at approximately 2.4 GHz remain unchanged, indicating that the lower mode is electrically isolated from variations in L_1.

Effect of Upper Strip Width (w_1): Modification of w_1 as shown in *figures 5(c)* and *5(d)* impacts the first resonant frequency (approximately 3.3GHz) through the creation of noticeable shifts in frequency and impedance mismatch, due to altering the capacitive loads at the top horizontal. In the ON state, w_1 mainly controls the first 'mode' of resonance only, while leaving the second resonance reasonably unaffected. This suggests a moderate degree of influence on tuning and impedance characteristics, particularly in multi-band antenna systems.

Effect of Central Slot Width (wd_1): The influence of the central slot width on the resonant behaviour of the antenna, shown in *figure 5(e)* and *figure 5(f)*, is due to the passive PIN diode with its reverse bias (R_off ≈ 5 KΩ). The remaining parasitic capacitance (C_off≈ 0.1 pF) across the open negative diode gap affects the coupling of the disconnected substrates with each other electromagnetically at all frequencies, mainly at low frequencies and affects both the depth and frequency of the first resonance [16], [17]. As wd1 increases, the central slot becomes wider, thereby allowing additional paths for surface currents and corresponding near-field distributions and leads to improved energy distribution and sharper values for return losses even though no conduction paths are present to complete the circuit. Thus, it emphasises the importance of retaining small dimensions in the central slot of a planar microstrip structure.

During its ON state, when the diode acts as a series inductor with low resistance, wd_1 has a much more direct effect on the second resonance allowing for improved impedance matching as well as increased tuning capability. The first resonance is mainly unaffected, which reinforces the fact that it is not dependent on the capacitive loading created by the center slot after the current paths of the elements have been unified. In addition, it can be shown that wd1 is vital for tuning in both the low and mid-frequency bands, depending on the bias condition of the diode. Consequently, optimizing wd_1 increases the antenna's coupling efficiency in the OFF mode and helps refine the matching in the ON mode contributing to an overall increase in the robustness and dependability of an antenna's multi-band performance.

Optimal Parameter Selection: The baseline parameters selected represented the most suitable set of options (L_1 = 7 mm, w_1 = 6 mm, wd_1 = 2.5 mm) from the parametric the trends indicated similar results for all performance parameters, yielding the greatest S_{11} depth, stable resonance, and adequate bandwidth in both modes of operation. The balance of each parameter is critical in order for the antenna to achieve appropriate levels of frequency reconfigurability and efficient matching, even with practical variations. In addition, the influence of L_1 on the highest frequency bands, of w_1 on the middle frequency bands, and of wd1 on the lowest frequency bands allows for precise targeting and fine-tuning of the design for specific frequencies. Based on the preceding analysis, we conclude that the analytical relationships presented in section2 were effective in determining the initial electrical dimensions of the proposed design, while the final values for L_1, w_1, and wd_1 were improved through CST-based optimization to achieve the multi-band performance described in this work.

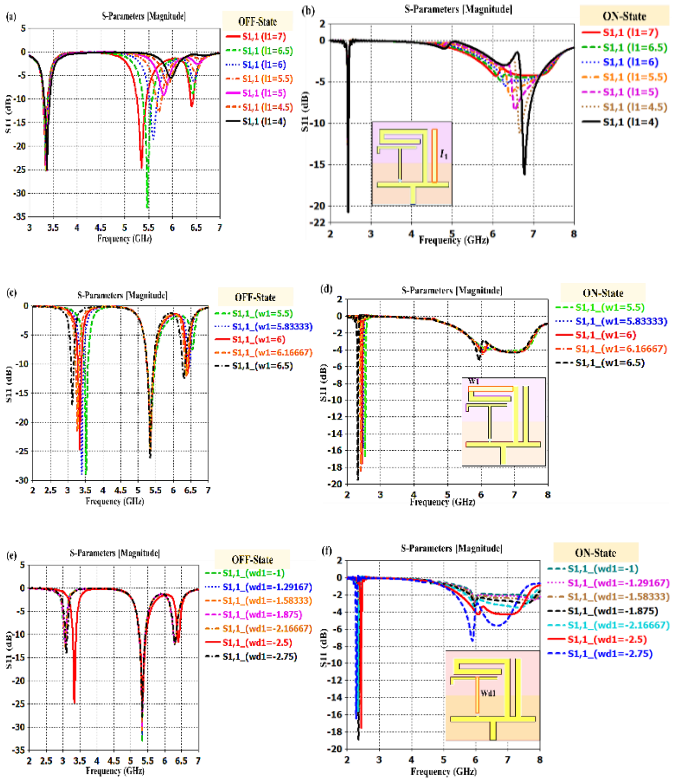

Figure 5. Effect of modifying stub length L_1, upper strip width w_1, and slot width wd_1 on Resonant Frequency and S_{11} in ON/OFF States

4.3. Reconfigurable Antenna Radiation Analysis: Gain, Directivity, VSWR, and Far-Field Patterns

The antenna's radiation performance was analyzed based on the central evaluation parameters (gain, directivity, and Voltage Standing Wave Ratio (VSWR) [18], [19], obtained from CST simulation results at all resonances and switching states as shown in *table 1* and *figures 6* to *figure 7* (the 3D radiation plot). These parameters verify that the antenna will function properly, through the electromagnetic mechanisms associated with the antenna's reconfigurable operation.

In the diode-OFF condition, where the switch behaves as an open circuit, the antenna reaches a peak gain of about 1.96 dBi at 5.347 GHz. This gain level is mainly due to the efficient excitation of a higher-order mode and the smoother flow of surface currents along the longer radiating paths. When the diode is switched to the ON state and presents a short circuit, the gain decreases to roughly 0.52 dBi at 2.44 GHz. This drop is linked to the modified current pattern and the stronger confinement of energy in the near field, which limits the amount

FOREX Publication
Open Access | Rapid and quality publishing
International Journal of Electrical and Electronics Research (IJEER)
Research Article | Volume 13, Issue 4| Pages 960-970|e-ISSN: 2347-470X

of power radiated into the far field. The lower gain at 2.44 GHz is also related to the antenna having a smaller electrical size at this frequency, which naturally restricts its effective aperture and radiated power an expected compromise in compact reconfigurable or wideband designs.

Directivity is a component of a wave's directional characteristic. Maximum directivity occurs when there is strong alignment among both the wave's electric field and current flows, which corresponds to an increase in the amount of energy confined within the narrowest space possible. Maximum directivity is evidenced by a value of 2.83 dBi at a frequency of 6.409 GHz, indicating an increased degree of interdependence and the presence of constructive interference of the EM fields of the radiating source. Beam narrowing and its relationship to other characteristics of RF propagation can facilitate focused wireless communications over short distances.

In both OFF and ON mode, high radiation efficiency has been consistently achieved regardless of state. The OFF mode has maximum efficiencies of 91.5% at 3.34 GHz and 91.3% at 5.347 GHz, which shows very low dielectric and ohmic loss due to very well matched impedances. Although the efficiency at the 6.409 GHz mark has dropped down to 78.1%, this is expected for higher order modes since the amount of surface wave leakage increases and the edge diffraction is greater. The ON mode has maintained an efficiency rating of 83.4% at the lower frequency of 2.44 GHz even though the gain has been reduced, which shows that the antenna transfers energy effectively and makes it applicable in energy constrained scenarios.

Table 1. Performance Metrics and Application Mapping for Reconfigurable States

Switching State	Frequency (GHz)	S_{11}(dB)	Peak Gain (dBi)	Realize Gain (dBi)	Directivity (dBi)	Radiation Efficiency (%)	VSWR	B.W (MHz)	Application Domain
OFF (Diode = Open)	3.34	-24.7	1.34	1.33	1.7	91.5	1.123	99	Sub-6 GHz 5G (n77/n78), WiMAX
	5.347	-24.6	1.98	1.96	2.35	91.3	1.124	203	Wi-Fi 5 (IEEE 802.11ac), ISM
	6.409	-11.6	1.88	1.75	2.83	78.1	1.71	55	WLAN (5.8 GHz), DSRC, satellite uplink
ON (Diode = Short)	2.44	-17.8	0.83	0.52	1.29	83.4	1.295	20	WLAN (IEEE 802.11b/g), Bluetooth, IoT

Across all operational bands, the VSWR values are less than 2 which demonstrates that good matching has been achieved with low return loss. The lowest VSWR is 1.123 at 3.34 GHz. This value shows that almost perfect matching exists and that the tuning using slots and stubs was successful in minimizing the interface mismatches providing optimal performance for maximum transmission efficiency in all reconfigured operational configurations.

Overall, the antenna presents stable radiation behavior and high efficiency across all reconfigurable states. Its operational profile is compatible with modern wireless communication standards, including 5G Sub-6 GHz (n77/n78), Wi-Fi (IEEE 802.11ac/b/g), Bluetooth, and IoT, making it a strong candidate for future multi-standard wireless platforms.

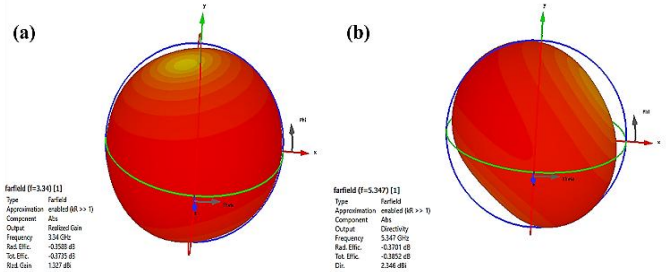

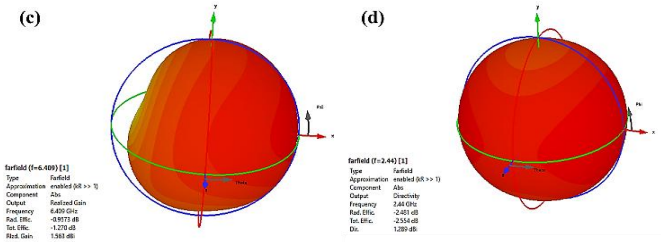

Figure 6. 3D Far-field radiation patterns at the resonant frequencies of the reconfigurable antenna in different switching modes. *(a)* Realized gain at 3.34 GHz (OFF state), *(b)* Directivity at 5.347 GHz (OFF state), *(c)* Realized gain at 6.409 GHz (OFF state), *(d)* Directivity at 2.44 GHz (ON state)

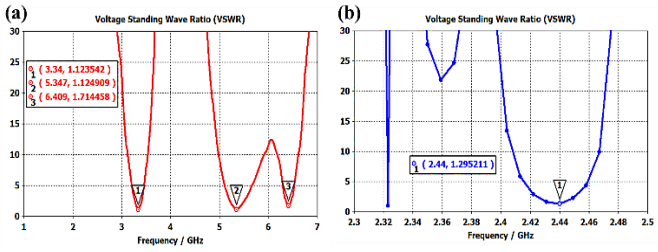

Figure 7. Simulated Voltage Standing Wave Ratio (VSWR) of the proposed reconfigurable antenna for both switching states: (a) OFF state (diode open); (b) ON state (diode shorted)

FOREX Publication
Open Access | Rapid and quality publishing
International Journal of Electrical and Electronics Research (IJEER)
Research Article | Volume 13, Issue 4| Pages 960-970|e-ISSN: 2347-470X

Radiation pattern analysis further substantiates these findings [18], [19]. The configuration of the OFF-state in *figures 8(a)–(c)* shows a beam tilt and a vertical concentration increase as the frequency increases. The angle of the beam has changed from 174° at 3.34 GHz to 165° at 6.409 GHz, which results from the phase difference with frequency along the edges of the patch. The pattern of the ON-state at 2.44 GHz appears more symmetrical than the OFF-state and has lower sidelobe levels, indicating larger area coverage with less backward radiation, which is important for low-interference IoT uses.

The Antenna has successfully achieved a very good balance between compact size, ability to be reconfigured, and radiation efficiency. The antenna has consistently provided good gain (directionality) and efficient impedance matching throughout all switching states of operation. As such, this antenna is ideal for use on Sub-6 GHz products including Wireless Local Area Networks, Bluetooth, and 5G low-band applications. Results from testing have shown that by designing the reconfiguration elements and tuning the geometrical configuration of the antenna, it is possible to create an antenna capable of adaptive function without losing radiation stability which is an essential feature of any modern day multi-functional wireless device.

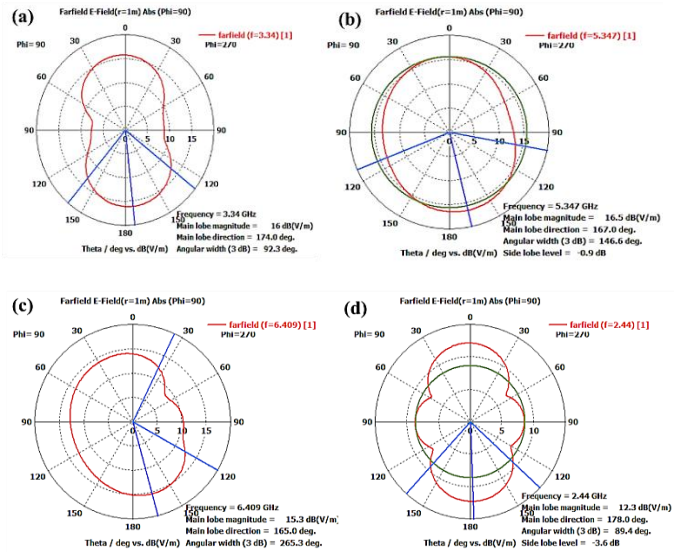

Figure 8. 2D E-plane radiation patterns at four resonant frequencies: (a) 3.34 GHz, (b) 5.347 GHz, (c) 6.409 GHz, and (d) 2.44 GHz

4.4. Surface Current Distribution

To understand the behavior and the efficiency of the antenna, the areas of current distribution and the important flow points between the feedline and the radiated patch should be analyzed [18], [19].

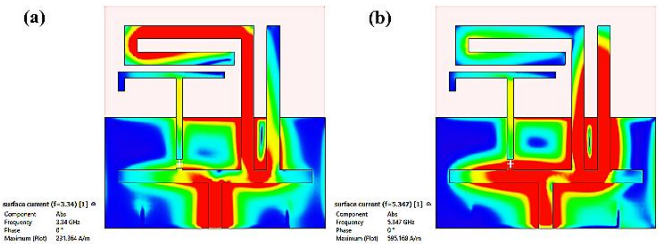

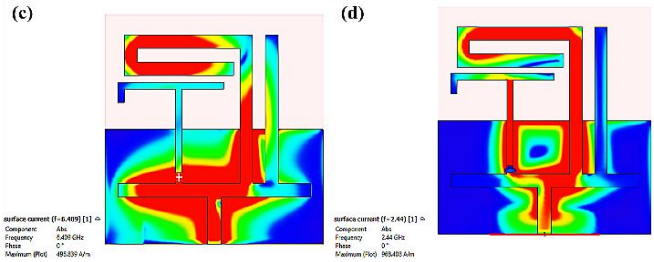

Figure 9. Simulated surface current distribution of the proposed antenna at (a) 3.34 GHz, (b) 5.347 GHz, (c) 6.409 GHz (OFF state), and (d) 2.44 GHz (ON state)

The surface current spread at the four resonant frequencies contribute to a better understanding of the antenna's reconfiguration mechanism, modal excitation behavior, and field confinement characteristics, as shown in *figure 9(a)-(d)*.

Strong surface currents are found circulating along the outer edge of the horizontal stub and on top left area of main radiator at 3.34 GHz (*figure 9(a)*). The length of these currents follows a quarter-wavelength resonance characteristic, supporting that the first resonance is due to the excitation of the longest current path in the OFF state. The maximum surface current is up to 231.364 A/m, which means that the antenna efficiently radiates at the Sub-6 GHz band.

At 5.347 GHz (see *figure 9(b)*), current flows to the middle of the inner vertical stub and the central feed area. This suggests the excitation of a higher-order mode supported in compact current loops and enhanced capacitive interaction at the diode interface. The existence of dense current at the vertical segment indicates strong coupling and high stored energy, which is in agreement with a measured peak gain of 1.96 dBi.

At 6.409 GHz (*figure 9(c)*) the surface current distributes on both vertical and lower arms. The peak is pronounced around the open-end slots and lower patch extensions, indicating a resonant behavior through high order hybrid modes and strong interface coupling. The current maximum value reaches 496.839 A/m, which explains the strong directivity (2.83 dBi) and good radiation efficiency obtained.

At 2.44 GHz (*figure 9(d)*), which is in the ON state, a huge re-distribution of surface currents takes place because of low resistance conduction path made available by forward biasing of diode. It's to be found that the current is focused in a newly connected central slot and lower stub section, giving rise to a compact, low frequency mode. It is remarkable to observe through surface current that current/energy all accumulates around a smaller space (presented as 968.408 A/m for the power confinement). This explains the lower peak gain (0.52 dBi) as proof of the successful reconfiguration which is represented by.

In other words, the different operational frequencies stimulate relatively independent current paths. The switching by the PIN diode causes an obvious topological transformation of current distribution, thus confirming its effective frequency agility and multi-band reconfigurability. The evolution of surface current tracks in OFF and ON state also evidences physical separation

FOREX Publication
Open Access | Rapid and quality publishing
International Journal of Electrical and Electronics Research (IJEER)
Research Article | Volume 13, Issue 4| Pages 960-970|e-ISSN: 2347-470X

between bands and the robustness of our design against electrical reconfiguration.

4.5. Statistical Tolerance Analysis Using Monte Carlo Simulation

Although Printed Circuit Board (PCB) prototyping tools are available locally, the fabrication of the proposed antenna was not carried out due to the limited availability of substrate thicknesses, restricted to only three standard options, and the absence of low-loss, high-frequency materials such as Rogers RT/Duroid. As the antenna design relies on a specific substrate type and thickness to achieve accurate impedance matching and stable resonant behavior, its physical implementation would require fabrication through specialised facilities abroad.

To resolve this limitation, a Monte Carlo simulation was implemented to inspect the design's behavior under typical fabrication errors [20], [21]. The results demonstrated that the antenna maintains stable electrical performance under reasonable dimensional deviations, thereby improving its manufacturability and reliability under appropriate industrial conditions.

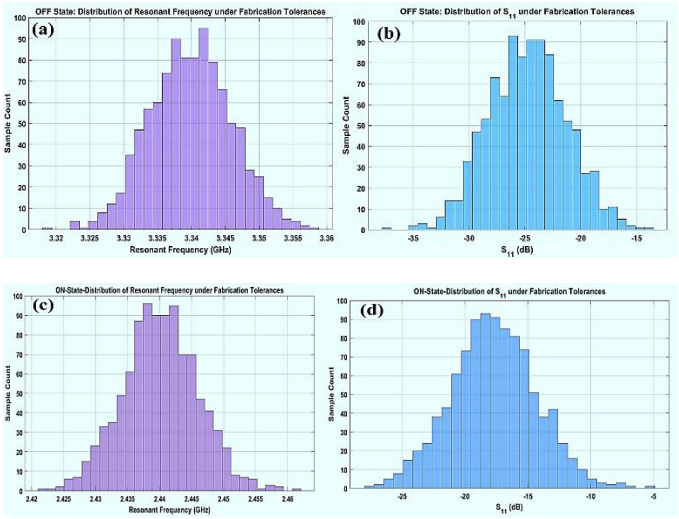

Figure 10. Monte Carlo-Based Statistical Evaluation of Resonant Frequency and Reflection Coefficient (S_{11}) under Fabrication Tolerances for Reconfigurable Antenna in ON and OFF States

The Monte Carlo simulation in *fig. 10* presents a statistical analysis of the sensitivity of the antenna to fabrication tolerances by considering 1000 random samples with different substrate thickness, copper layer and trace width. Such an analysis is very important because there are no physical prototypes and the result could give insight on the robustness of the design and control loop versus manufacturing variations.

In its OFF state the resonant frequency (*fig. 10(a)*) and is significantly clustered around 3.34 GHz ($\sigma = \pm 0.005$ GHz). This narrow spread indicates that the antenna basic mode, is established through stable electromagnetic paths barely affected by minor geometrical perturbations. Similarly, the reflection coefficient (*fig. 10(b)*) shows the strong clustering at about −24.7 dB, which implies that the impedance matching was quite robust with respect to fabrication parameters variations. This is due to the regulated geometry and isolation of first mode in structure with components since it is more sensitive to parasitic loading.

When the device is in ON state, resonance frequency [Fig. 10 (c)] is observed to have a centered distribution at 2.44 GHz with the same similar stability level. While the diode based current path changes the effective electrical length, its confinement results in little dispersion. The S_{11} variation [Fig. 10 (d)] is –17.8 dB, and no outliers over the matching threshold at –10 dB are found, indicating that reliable return loss can be achieved in a reconfigured operation mode.

The findings provide confirmation of two critical attributes of the antenna design: Fabrication tolerance immunity means that through practical variations in manufacturing, the performance of the antennas should continue to mimic what is expected from the design, thereby minimizing the chances of detuning or degradation of operating characteristics in production. Design maturity and manufacturability, indicated by the statistical similarity (both on/off) of both S_{11} and resonant frequencies suggests that the antennas are both electromagnetically reliable and easily produced based on the assumption that the required substrate materials are available.

Essentially, Monte Carlo analysis can be used as a means to pre-evaluate the simulation design and increase the confidence of the simulation's ability to function as intended over an acceptable range. The analysis also assures that the simulated design can operate within acceptable parameters of safety when produced by standard processes.

5. COMPARATIVE ANALYSIS

Researchers have been prompted to develop reconfigurable antenna designs that offer compactness, while still providing high radiation efficiency to support the technological advancements of compact wireless systems and the growing demand for frequency-agile antennas used in new Sub-6 GHz applications (5G, WLAN, IoT). In this paper, we will present a small reconfigurable antenna with stable performance in both ON and OFF switch modes and with the ability to provide different operating frequencies. It also provides consistency in radiation pattern.

The proposed antenna employs one PIN diode to dynamically control the operational modes of the antenna. This is in contrast to many of the previously published designs which could not be configured with just one switch due to complicated geometries. The simplicity of the proposed design enhances the reliability of the design and reduces fabrication costs. In addition, the proposed design strikes an acceptable balance between gain, bandwidth and directionality.

Table 2 presents a comparative summary of the proposed antenna against several state-of-the-art reconfigurable designs reported in the literature. The comparison highlights key performance indicators, including the number of bands, resonant frequencies, realized gain, switching mechanism, and physical dimensions. It is evident from the analysis that the

FOREX Publication
Open Access | Rapid and quality publishing
International Journal of Electrical and Electronics Research (IJEER)
Research Article | Volume 13, Issue 4| Pages 960-970|e-ISSN: 2347-470X

proposed design achieves competitive or superior metrics in terms of compactness, dual-mode operation, and suitability for low-power wireless devices.

The comparative results presented in Table 2 clearly highlight the practical advantages of the proposed design over prior reconfigurable antennas. In terms of dimensional compactness, the proposed antenna measures only 17 × 17 × 0.55 mm³, making it the most space-efficient among the surveyed designs. This footprint is notably smaller than all previous work and further improves upon the miniaturization reported in [10] (15 × 21 × 1.6 mm³), especially when considering the significantly thinner substrate used. This physical reduction facilitates easier integration into portable and embedded platforms, a critical requirement for modern WLAN, IoT, and Sub-6 GHz 5G modules.

From the perspective of switching complexity, most existing works employ multiple PIN diodes, up to four in [22], [23], and [11] to achieve frequency reconfigurability. Such configurations introduce increased power consumption, control circuitry overhead, and higher insertion loss. In contrast, the proposed antenna utilizes only a single PIN diode to dynamically switch across four operating bands (2.44, 3.34, 5.347, and 6.409 GHz), offering an elegant solution that significantly reduces hardware complexity without compromising functional flexibility. Among the surveyed designs, only [24] employs a similarly minimal switch configuration (1 diode), yet it supports only two bands.

Table 2. Comparative Evaluation of the Proposed Antennas against State-of-the-Art Designs

References	Dim. (mm³)	Substrate	No. of switches	Operating band number	Operating Frequency (GHz)	Peak Gain (dBi)	Radiation Efficiency (%)
[22]	37.8×40.4×1.6	FR-4	4-PIN diode	2	2.4, 5.6	1.92	-
[23]	40 × 32 ×1.6	FR-4	4-PIN diode	9	1.8, 2.1, 2.6, 3.5, 4.8, 5.0, 5.6, 6.4, 6.5	1.25–3.6	71-84
[9]	35×35×1.6	FR-4	3-PIN diode	5	5.8,4.7,3.5,2.4, 6.23	2.3-4.91	73-79
[10]	15 × 21 × 1.6	FR-4	2-PIN diode	6	7.3, 2.55, 5.3, 3.36,7.3,5.4	2.07-3.38	-
[11]	22 × 22 × 0.762	RT/duroid 5880	4-PIN diode	13	7.25, 7.5, 8.1, 8.2, 8.7, 9.2, 10, 11.5, 11.9, 12.1, 12.2,13.4, 13.5	5.34	63.39-87.75
[24]	20 × 15 × 1.4	FR-4	1-PIN diode	2	6.04,2.4	4.82	-
This Work	17 × 17 × 0.55	RT/duroid 5880	1-PIN diode	4	3.34,5.347,6.409,2.44	0.83-1.98	83.4-91.5

Regarding operating frequency coverage, the proposed antenna provides a balanced spread of four discrete bands across low, mid, and high Sub-6 GHz ranges, encompassing major wireless communication protocols. While [23] and [11] achieve broader multi-band operation with 9 and 13 bands, respectively, this comes at the cost of higher switching demands and degraded radiation efficiency. For example, [23] reports efficiencies of 71–84%, and [11] exhibits a wider range of 63.39–87.75%, both of which remain lower than the proposed design's consistent 83.4–91.5% efficiency across all bands.

In terms of gain, the proposed antenna demonstrates values ranging between 0.83 and 1.98 dBi, which are acceptable for short-range, low-power wireless applications. Although higher peak gains are reported in [11] (5.34 dBi), [9] (up to 4.91 dBi), and [24] (4.82 dBi). These designs require larger physical areas and more complex switching networks, which may limit their suitability for compact or energy-constrained systems. Moreover, [22] and [23], despite using four switches, exhibit relatively modest gains (1.25–3.6 dBi), suggesting inefficiencies in radiative performance despite increased hardware complexity.

Additional differences from other designs are seen in the selection of substrate material. Previous designs have predominantly employed FR-4, which is an economical method but contains a material that suffers from large dielectric loss, limiting both efficiency and usable bandwidth. The design of the proposed antenna, utilizing RT/Duroid 5880 as the substrate material, provides substantial benefits to performance evidenced by the very low levels of return loss and the high efficiency of the proposed antenna radiating across its complete operating frequency range.

As a whole, The comparative analysis shows that the new design of the Antenna achieves the best balance over all major design criteria; it provides a small form factor, a low number of switches, stable multi-band operation, good efficiency and reasonable gain all this adds up to being the best option for the next-generation wireless applications, where space, power, and spectral efficiency play a vital role.

The outcome of this work shows that the folded T-stub topology, combined with a simple PIN-diode switching mechanism, can provide for a controlled and predictable transition between multiple operating bands without resorting to complicated reconfigurable structures. The behavior followed in all the simulations indicates that no single resonant path dominates in the antenna but rather a combination of various current trajectories contributes simultaneously,

explaining the stability of resonances under dimensional variations and switching states. Further, the results indicate that electromagnetic coupling between the stub sections and the modified ground plane represents the critical factor governing the separation and robustness of operating bands. This proves that the proposed configuration ensures functional consistency even when compacted to a very small footprint, a requirement crucial for modern Sub-6 GHz wireless devices. The overall result of the work presents a compact, easily tunable antenna architecture that offers reliable multi-band behavior with minimum circuitry and without sacrificing impedance performance.

6. CONCLUSIONS

The investigations presented in this work demonstrate that the folded T-stub configuration, along with a single PIN-diode switching element, provides an effective and technically mature solution to attain predictable multiband reconfigurability within a compact antenna footprint. The intentional folding of the radiator and the consequential capacitive discontinuities are central in the derivation of the current distribution and play a key role in deciding the separation and stability of the supported resonant modes. With this mechanism, transitions between the operating bands can be reliably achieved without resorting to multi-diode networks or geometrically complicated reconfigurable structures. The electromagnetic behavior across the different configurations demonstrates that the proposed design maintains consistent impedance characteristics and robust modal stability under structural variations, which underlines its suitability for integration into size-constrained Sub-6 GHz devices. Besides offering a practical pathway to low-cost, energy-efficient, and easily deployable reconfigurable front-end solutions for next-generation multi standard wireless communication platforms, these antenna structures effectively combine structural simplicity with controlled electromagnetic behavior. Overall results emphasize the value of the folded T-stub approach as a compact and reliable design strategy for modern RF systems.

REFERENCES

[1] D. N. Gençoğlan, Ş. Çolak, and M. Palandöken, "Spiral-Resonator-Based Frequency Reconfigurable Antenna Design for Sub-6 GHz Applications," Applied Sciences (Switzerland), vol. 13, no. 15, 2023, doi: 10.3390/app13158719.

[2] A. Kumar, M. Aljaidi, I. Kansal, K. Alshammari, G. Gupta, and S. M. Alenezi, "Recent Trends in Reconfigurable Antennas for Modern Wireless Communication: A Comprehensive Review," Int J Antennas Propag, vol. 2024, no. 1, Jan. 2024, doi: 10.1155/ijap/8816812.

[3] A. Tiwari, G. K. Soni, D. Yadav, S. V. Yadav, and M. V. Yadav, "Rectangular loaded ring-shaped multiband frequency reconfigurable defected ground structure antenna for wireless communication applications," Results in Engineering, vol. 25, p. 104339, Mar. 2025, doi: 10.1016/j.rineng.2025.104339.

[4] M. S. Yahya, S. Soeung, S. K. A. Rahim, U. Musa, S. S. Ba Hashwan, and M. A. Haque, "Machine Learning-Optimized Compact Frequency Reconfigurable Antenna with RSSI Enhancement for Long-Range Applications," IEEE Access, vol. 12, 2024, doi: 10.1109/ACCESS.2024.3355145.

[5] T. K. Nguyen, C. D. Bui, A. Narbudowicz, and N. Nguyen-Trong, "Frequency-Reconfigurable Antenna with Wide- and Narrow-band Modes for sub-6 GHz Cognitive Radio," IEEE Antennas Wirel Propag Lett, 2022, doi: 10.1109/LAWP.2022.3201969.

[6] M. Kaur, H. Shankar Singh, and M. Agarwal, "A compact two-state pattern reconfigurable antenna for 5G Sub-6 GHz cellular applications," AEU - International Journal of Electronics and Communications, vol. 162, 2023, doi: 10.1016/j.aeue.2023.154577.

[7] S. Shrimal, R. Agrawal, I. B. Sharma, and M. M. Sharma, "Dual wideband circularly polarized reconfigurable antenna using gap loaded annular ring," AEU - International Journal of Electronics and Communications, vol. 178, p. 155296, May 2024, doi: 10.1016/j.aeue.2024.155296.

[8] T. K. Nguyen, C. D. Bui, A. Narbudowicz, and N. Nguyen-Trong, "Frequency-Reconfigurable Antenna with Wide- and Narrowband Modes for Sub-6 GHz Cognitive Radio," IEEE Antennas Wirel Propag Lett, vol. 22, no. 1, pp. 64–68, Jan. 2022, doi: 10.1109/LAWP.2022.3201969.

[9] K. Thenkumari, K. S. Sankaran, and J. M. Mathana, "Design and Implementation of Frequency Reconfigurable Antenna for Wi-Fi Applications," Engineered Science, vol. 23, 2023, doi: 10.30919/es8d876.

[10] O. Benkhadda et al., "A Miniaturized Reconfigurable Antenna for Modern Wireless Applications with Broadband and Multi-band Capabilities," Progress in Electromagnetics Research M, vol. 127, pp. 93–101, 2024, doi: 10.2528/PIERM24042801.

[11] A. Tiwari, G. K. Soni, D. Yadav, S. V. Yadav, and M. V. Yadav, "Rectangular loaded ring-shaped multiband frequency reconfigurable defected ground structure antenna for wireless communication applications," Results in Engineering, vol. 25, p. 104339, Mar. 2025, doi: 10.1016/j.rineng.2025.104339.

[12] A. Reha, O. Benkhadda, A. Oulad Said, A. El Amri, and A. Jamal Abdullah Al-Gburi, "Design of Sub-6GHz and Sub-7GHz DRAGON Fractal Antenna for 5G Applications with Enhanced Bandwidth," International Journal of Intelligent Engineering and Systems, vol. 18, no. 2, pp. 14–22, Mar. 2025, doi: 10.22266/ijies2025.0331.02.

[13] D. M. Pozar, Microwave Engineering, 4th Edition. 2012.

[14] C. A. Balanis, Antenna Theory: Analysis and Design, Wiley., vol. 4. 2016.

[15] N. Ahmed Malik, "Design of Implantable Antennas for Biomedical Applications," PhD, University of Bedfordshire., 2022.

[16] Boyapati Bharathidevi and Jayendra Kumar, "Effect of PIN Diode Integration on Patch Antennas for Frequency Reconfigurable Antenna Applications," Advances in Technology Innovation, vol. 8, no. 3, pp. 210–218, Jul. 2023, doi: 10.46604/aiti.2023.9235.

[17] M. Joler and J. Kucan, "Impact of Slot Parameters on the Three Resonant Frequencies of a Rectangular Microstrip Antenna: Study of the impact of the slot length, width, and position," IEEE Antennas Propag Mag, vol. 57, no. 4, pp. 48–63, Aug. 2015, doi: 10.1109/MAP.2015.2453888.

[18] J. N. Shehab, M. J. Farhan, and S. Al-Azawi, "A non-invasive wearable microwave sensor for Alzheimer's Stage differentiation using realistic 3D human head phantoms," Results in Engineering, vol. 27, p. 106350, Sep. 2025, doi: 10.1016/j.rineng.2025.106350.

[19] J. N., F. M. J. A.-A. S. Shehab, "Microwave Sensing System and Six-layer Phantom Model for Detection of Benign and Malignant Brain Tumors in Experimental and Simulated Environments," International Journal of Intelligent Engineering and Systems, vol. 18, no. 4, pp. 571–584, May 2025, doi: 10.22266/ijies2025.0531.37.

[20] W. Xu, K. Wu, and P. Li, "Monte Carlo Tolerance Analysis of Antennas /Radomes with Mesh/Element Strip Grouping," in 2021 IEEE International Symposium on Antennas and Propagation and USNC-URSI Radio Science Meeting (APS/URSI), IEEE, Dec. 2021, pp. 1253–1254. doi: 10.1109/APS/URSI47566.2021.9703733.

[21] S. Babu and G. Kumar, "Reliability Studies of Microstrip Antennas using Monte Carlo Simulation," IETE Technical Review, vol. 18, no. 1, pp. 51–56, Jan. 2001, doi: 10.1080/02564602.2001.11416943.

[22] P. Kumar, S. Dwari, R. K. Saini, and M. K. Mandal, "Dual-Band Dual-Sense Polarization Reconfigurable Circularly Polarized Antenna," IEEE Antennas Wirel Propag Lett, vol. 18, no. 1, pp. 64–68, Jan. 2019, doi: 10.1109/LAWP.2018.2880799.

International Journal of
Electrical and Electronics Research (IJEER)
Research Article | Volume 13, Issue 4| Pages 960-970|e-ISSN: 2347-470X

[23] H. Dildar et al., "Design and Experimental Analysis of Multiband Frequency Reconfigurable Antenna for 5G and Sub-6 GHz Wireless Communication," Micromachines (Basel), vol. 12, no. 1, p. 32, Dec. 2020, doi: 10.3390/mi12010032.

[24] A. H. Ali et al., "A compact dual-band reconfigurable antenna with metamaterial for IoT applications," Sci Rep, vol. 15, no. 1, p. 21039, Jul. 2025, doi: 10.1038/s41598-025-05174-y.